

# Wear Behavior of Brass Based Composite Reinforced with SiC and Produced by Stir Casting Process

E. Mohan<sup>a\*</sup> , G. Anbuezhiyan<sup>b</sup>, R. Pugazhenti<sup>c</sup>, F. Peter Prakash<sup>d</sup>

<sup>a</sup>Shanmuganathan Engineering College, Department of Mechanical Engineering, Pudukkottai, India.

<sup>b</sup>Saveetha Institute of Medical and Technical Sciences, Saveetha School of Engineering,  
Department of Mechanical Engineering, 60125, Chennai, India.

<sup>c</sup>Vels Institute of Science, Technology & Advanced Studies, Department of Mechanical Engineering,  
Chennai, India.

<sup>d</sup>Mount Zion College of Engineering and Technology, Department of Mechanical Engineering,  
Pudukkottai, India.

Received: April 13, 2022; Revised: February 16, 2023; Accepted: March 01, 2023

The current investigation presents the wear-worn surface analysis of a silicon carbide-reinforced brass-based composite synthesized by stir casting. Wear behavior of the brass composite pin was analyzed by disc tribometer. Wear characterization studies and confirmation of elemental composition are investigated through scanning electron microscopy (SEM) and energy dispersive spectroscopy (EDS) respectively. The worn surface of the synthesized brass composite was analyzed using atomic force microscopy (AFM). The aim of the investigation is to examine the surface morphology of the worn specimen. Based on the input constraints, the wear rate ranges from 0.0135 to 0.0893 mm<sup>3</sup>/min. The applied load is the predominant factor in the wear rate (83.75%). Sliding velocity has a minor effect on wear rate (1.06%). The improved surface roughness of 15.27 nm was produced on the worn surface. The novelty of the research work is to study the various surface parameters of the worn surface, such as roughness average, root mean square roughness, maximum height of the roughness, skewness, and kurtosis. These parameters were analyzed at different wear-worn surfaces of the synthesized brass composite. The wear-worn surface was deeply investigated and incorporated with SEM and AFM analysis.

**Keywords:** Brass composite, Silicon carbide, Wear characterization, Wear worn surface, Atomic force microscopy.

## 1. Introduction

Wear and strength play an essential role in materials and composites. Brass is stronger and stiffer than copper. It has excellent corrosion resistance, malleability, and formability characteristics. Brass and its alloys are used in gears, valves, bearings, couplings, and electrical and electronic components. It has a tensile strength of 39 Kg/mm<sup>2</sup>, Vickers hardness of 105, and a density of 84 kg/mm<sup>3</sup><sup>1</sup>. The brass alloy has an exceptional abrasive wear rate and frictional behavior. An abrasive wear rate of 0.0003 mm<sup>3</sup>/Nm was attained at 50 N of load for brass<sup>2</sup>. Friction coefficient and wear behavior experiment was conducted on the brass alloy. It was observed that sliding velocity played an essential role in wear rate<sup>3</sup>. In the wear behavior of copper and brass alloys, the coefficient of friction decreases as the applied load increases. SiC reinforcement particles were used to enhance the tribological and material properties<sup>4</sup>. The wear rate mainly depends on the weight percentage of the reinforcement particles and the material properties. It was concluded that the wear layer was found on the surface of the duplex brass<sup>5</sup>. Wear and strength are the essential material properties of

the composite. The volume fraction of reinforcement and its effect on wear rate were analyzed under different temperature conditions<sup>6</sup>. The wear experimentation was conducted on a titanium carbide-based copper composite. The influential factor and its role in wear rate were analyzed<sup>7</sup>. Reduction in grain size and the accumulation of reinforcement increased the material's properties and wear resistance in copper composite<sup>8</sup>. The wear behavior of the copper composite was analyzed under different input constraints. The disc rotational speed produced a major effect on wear rate<sup>9</sup>. Wear rate and coefficient of friction were evaluated for different compositions of copper composite. The wear surface of the copper composite under different load conditions was analyzed by scanning electron microscope images<sup>10</sup>. Wear volume and wear rate were decreased by an applied load of 20N. The coefficient of friction was decreased by the increase of reinforced particles in the brass alloy. Delamination of wear particles and debris was observed in the wear test on brass<sup>11</sup>. Mechanical and wear behaviors were investigated in the sandblasting and annealing processes of a brass alloy. The grain size of the reinforced particle had the greatest influence on the wear rate in brass alloy<sup>12</sup>. The purpose of the

\*e-mail: mohanmechmz@gmail.com

present article was to investigate the worn surface on brass composites produced by the stir casting process. The alloying composition and characterization of the composite were confirmed by EDS and SEM. The wear-worn surface analysis on the brass composite was conducted by AFM analysis.

## 2. Materials and Methodology

### 2.1. Raw material

Copper and zinc are the main compositions of pure brass. It is lead-free brass, and it is considered for experimental investigation. It is more malleable than other materials, and it has exceptional material properties. It consists of 66% copper and 34% zinc. The brass billets are purchased from NEXTGEN Metals in Mumbai, India. The total weight of the raw material is around 4 kg, and the diameter is 1 inch. Between copper and zinc, silicon carbide acts as reinforcement. It has outstanding hardness and mechanical strength at elevated temperatures, higher thermal conductivity, and corrosion and oxidation resistance.

### 2.2. Sample preparation

A silicon carbide-reinforced brass-based composite was synthesized by the stir casting technique. It is an exceptional and popular technique for developing reinforced composite materials. The reinforcement phase and uniform mixture of molten metal play an essential role in the stir-casting process. A muffle furnace preheats the SiC particles at 1500 °C for 50 minutes. A graphite crucible furnace develops the melts from brass (69 wt.% of copper and 29.5 wt.% of zinc) with silicon carbide particles (1.5 wt.%). The stirrer was applied to the molten metal at 600 rpm. Silicon carbide particles with a size of 20  $\mu\text{m}$  were chosen. The preheated silicon carbide particles were placed into the molten metal and stirred at 700 rpm for 20 minutes. Figure 1 clearly depicts the shape morphology of SiC particles. The molten metal was poured into the cast iron mould. After the solidification process, the metal part was removed and machined to 50 mm in length and 10 mm in diameter.

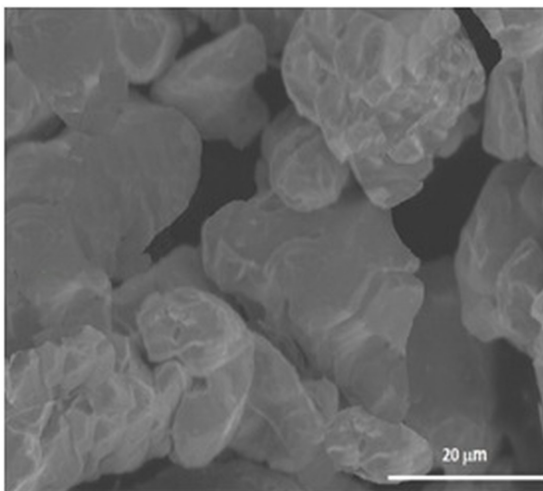


Figure 1. SEM image of SiC particles.

### 2.3. Characterization of the brass composite

The characterization of the synthesized brass composite is shown in Figure 2. From the figure, it was observed that the SiC particles are entrenched on the brass composite and uniformly spotted over the surface due to the least amount of the reinforced particles, as was clearly shown in Figure 2.

### 2.4. Description of wear and material test

The wear characteristics were analyzed by a pin-on-disc tribometer. The pin was made of brass composite with a 10 mm diameter and 20 mm height. The ASTM G-99 standard was used to follow the wear test. Initial roughness of the pin is 11.2 nm. It was measured by surface roughness tester. Various sizes of emery paper were used to finish the pin surfaces, which were cleaned carefully with an acetone solution. EN-31 steel was used as the disc material. As per the ASTM E8 M11 standard, the specimens were prepared. The total length of the specimen is 50 mm, with front and back end diameters of 10 mm. The neck diameter is 6 mm, and the length is 30 mm was fabricated for the tensile test. A Brinell hardness tester with a ball diameter of 10 mm and a load of 500 kgf was used. The test results noted that the composite has better material properties, such as a hardness of 510 BHN, a density of 8.6 g/cc, and a tensile strength of 475 MPa. AFM (OEM model, Korea) deeply analyzed the worn surface of the brass composite. The scanning resolution is 0.2 nm in the XY direction and 0.05 nm in the Z direction. AFM is the best tool to provide information about surface topography parameters. The scan size of 100 mm by 100 mm was used in the atomic microscope to study the roughness parameters. Imaging software was involved in calculating the roughness parameters. The chemical composition ensured by EDS is shown in Figure 3. EDS (Carl Zeiss, Jena, Germany) with sensor active areas of 10mm<sup>2</sup> to 100mm<sup>2</sup> and a resolution of 123–133 eV was used. The primary composition of the composite is copper and zinc.

## 3. Result and Discussion

Experimental results for frictional wear are shown in Table 1. The sliding distance and track diameter for the entire test are

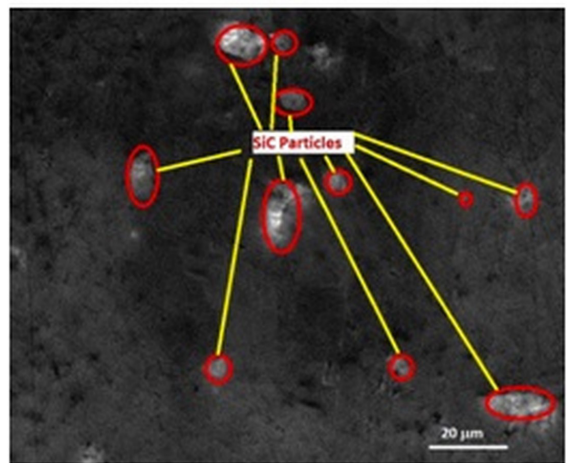


Figure 2. SEM image of the brass composite.

kept constant (18 m and 100 mm, respectively). Different control factors and their levels were used to evaluate the wear rate. The various input constraints and their levels are 15–25 N of applied load, 400–1200 rpm of disc rotational speed, and 3–9 m/s of velocity. Equation 1 was used to evaluate the wear rate. Standard deviation of the wear rate is 0.0237

$$\text{Wear rate} = \text{Volume of wear loss} / \text{applied load} \times \text{sliding distance} \quad (1)$$

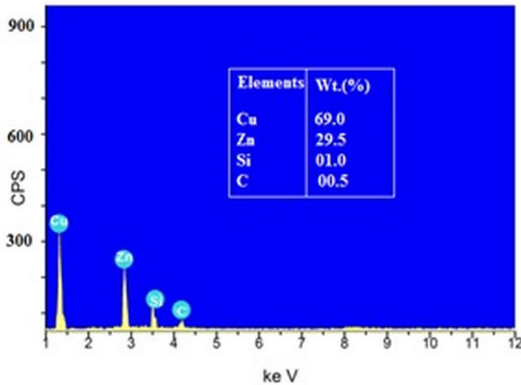


Figure 3. EDS image of brass composite.

Figure 4a-4b describe the wear rate of the brass composite samples concerning velocity and disc speed. Figure 4a demonstrates the wear rate as a function of velocity for the different loads, such as 15N, 20N, and 25N. This figure confirms that the low wear rate was perceived (0.0135 mm<sup>3</sup>/min). The maximum wear rate was attained at a load of 20 N and a sliding velocity of 6 m/s. It was observed that the samples were quickly worn and had a wear loss of 0.0893 mm<sup>3</sup> due to severe abrasive action<sup>13,14</sup>. Figure 4b illustrates the composite's wear rate as related to disc speed and load condition. The figure clearly stated that the wear rate gradually increased with an increase in disc rotational speed. More rubbing action was observed due to the temperature that developed between the contact surfaces of the pin and disc<sup>15</sup>. Owing to high disc speeds, sudden increases in temperature cause a decrease in the specimen's strength and wear<sup>16</sup>. It was interesting to note that the wear rate gradually increased from 400 rpm to 1200 rpm. It was concluded that the 34% wear rate had increased from 400 rpm to 1200 rpm. The minimum wear rate of 0.0587 mm<sup>3</sup>/min was attained at maximum load conditions. The variance analysis of frictional wear is shown in Table 2. The wear rate of the brass composite depended on the different input constraints. Rubbing action was increased with an increase in load. The load developed the most elevated effect on

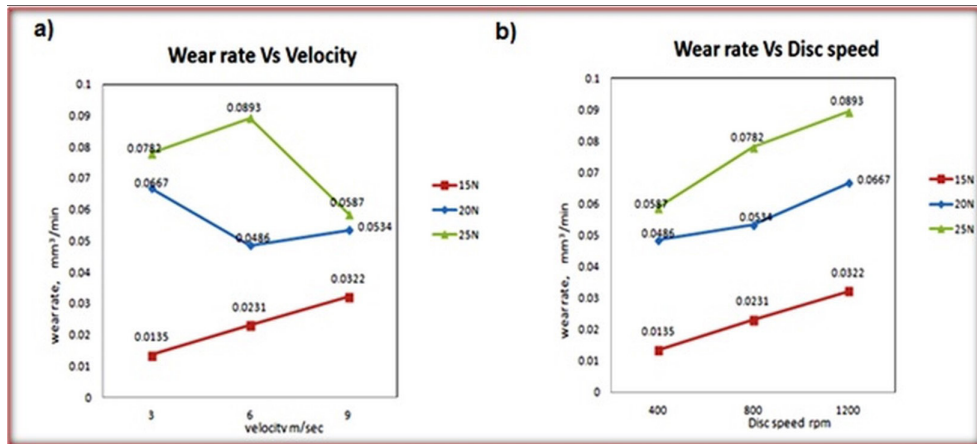


Figure 4. Wear rate of the samples a) function of velocity b) function of disc speed.

Table 1. Experimental results for wear rate of brass composite.

S.No	Load (N)	Disc speed (rpm)	Velocity (m/s)	Wear rate (mm <sup>3</sup> /min)
1	15	400	3	0.0135
2	15	800	6	0.0231
3	15	1200	9	0.0322
4	20	400	6	0.0486
5	20	800	9	0.0534
6	20	1200	3	0.0667
7	25	400	9	0.0587
8	25	800	3	0.0782
9	25	1200	6	0.0893

Standard deviation of the wear rate = 0.0237

**Table 2.** Variance analysis for wear rate.

Basis	DF	SS	MS	F	P	%
Load	2	0.004229	0.002115	214.57	0.005	83.57
Disc speed	2	0.000757	0.000379	38.42	0.025	14.96
Velocity	2	0.000054	0.000027	2.73	0.268	01.06
Error	2	0.000020	0.000010	----	----	00.41
Total	8	0.005060	---	----	----	100

wear rate among all the input constraints. It has produced an 83.75% effect on wear rate. The bonding strength between the surface layers was unstable and increased with the loss of materials<sup>17</sup>. The attained R squared, adjusted R squared, and predicted R squared are all greater than 90%. The disc speed and velocity contributions to wear rate are 14.96% and 1.06%, respectively.

### 3.1. SEM analysis

The worn surface of the brass composite was analyzed by scanning electron microscopy with varying loading conditions. SEM images of the specimen under different wear and load conditions were neatly demonstrated in Figure 5a-5e. From the figure, it has been confirmed that silicon carbide particles are scattered over the specimen. The wear debris spread over the surface due to the localized heat of the pin and abrasive wear. The amount of heat generation depends on the frictional force between the tool and the workpiece<sup>18</sup>. It was also demonstrated in a wear study by silicon particles being separated across the surface due to increased friction between the two surfaces<sup>19,20</sup>. The wear rate has increased without the addition of SiC particles in a brass alloy. The addition of SiC particles manipulates properties such as density and hardness in the brass<sup>21</sup>. Figure 5a shows the wear-worn surface at 25 N of load, 400 rpm of disc speed, 9 m/s of velocity, and a wear rate of 0.0587 mm<sup>3</sup>/min. Wear debris was found on the surface. Figure 5b shows the wear-worn surface at 20 N of load, 800 rpm of disc speed, 9 m/s of velocity, and a wear rate of 0.0534 mm<sup>3</sup>/min. Wear tracks and delamination of the wear layer were observed on the surface. Figure 5c shows the wear-worn surface at 15N of load, 400 rpm of disc speed, 3 m/s of velocity, and a wear rate of 0.01355 mm<sup>3</sup>/min. The pin profile on the surface produced the wear track lines. Figure 5d established the wear-worn surface at 20 N load, 400 rpm disc speed, 6 m/s of velocity, and a wear rate of 0.0486 mm<sup>3</sup>/min. The penetration of the wear track lines and localized positions of silicon particles were observed on the surface. Figure 5e shows the wear-worn surface at 25 N of load, 1200 rpm of disc speed, 6 m/s of velocity, and a wear rate of 0.0893 mm<sup>3</sup>/min. The impact of the pin produced wear penetration, and resistance against load was observed. Figure 5e revealed the wear-worn surface at 25 N of load, 1200 rpm of disc speed, 6 m/s of velocity, and a wear rate of 0.0893 mm<sup>3</sup>/min. The impact of the pin produced wear penetration, and resistance against load was observed.

### 3.2. AFM analysis

AFM analysis is the best approach to visualize the surface characteristics of the worn-out specimen. The atomic force microscopic image of the specimen was significantly employed to identify the surface characteristics, and it

clearly examined how the surface was damaged owing to the speed, load, and velocity throughout the wear test. It was principally focused on studying and clearly assessing the surface topography of the material. In the current study, AFM measurement is critical in associating surface characteristics such as roughness average, root mean square roughness, maximum height of the roughness, maximum roughness peak height, skewness, and kurtosis with the load value, sliding velocity, and disc speed in the wear test analysis. From Table 1, It was clearly stated that at the maximum load, disc speed, and velocity condition, a greater wear rate of 0.0893 mm<sup>3</sup>/min was recorded. It was likewise duplicated in the AFM measurement of the specimen 5, which has a maximum roughness peak height of 188.5 nm, a roughness average value of 43.12 nm, and a maximum root mean square value of 56.76 nm. At the same time, a minimum wear rate of 0.01355 mm<sup>3</sup>/min was clearly apparent on Specimen 3 at the conclusion of the wear test. The average roughness maximum root mean square roughness value, which has also been connected with the AFM measurement, has a lower value when compared to the other specimens in the surface Investigation. The worn surface of the brass composite has different shapes of cliffs and valleys. Average roughness, root mean square roughness, the maximum height of the roughness, roughness valley depth, peak height, skewness, and kurtosis were neatly delivered in Table 3. Figures 6-10 show 3D atomic force microscope images of the specimen under various wear and load conditions. The line profile, which depicts the texture, waviness, and surface roughness of the material, is also shown near the 3D AFM images. Table 3 shows that specimen 5 has the highest average roughness value of 43.12 nm, while specimen 3 has the lowest average roughness value of 15.27 nm. The root mean square value of 56.76 nm is also the highest in specimen 5 and the lowest in specimen 3. Kurtosis is another important parameter to use to characterize the surface of the specimen; if the value is less than 3, the surface seems to be flat; if it is greater than 3, the surface has a strong spike-like peak profile. The greatest value of kurtosis was clearly stated to resemble a spike profile on the surface<sup>22</sup>. In this study, specimen 3 with a wear load condition of 25 N produced a higher waviness profile, as seen in Figure 8. The root mean square value and maximum height of the roughness for the specimen 5 are 56.76 nm and 376.9 nm, respectively, which create a rougher surface<sup>23</sup>. Similar to the investigation<sup>24</sup>, negative skewness indicates less spiky surfaces, as is obviously indicated in Figure 6, and a higher skewness value evidently indicates hill-like surface morphology, as is clearly shown in Figure 7. From the research study in<sup>25</sup>, the ratio of the

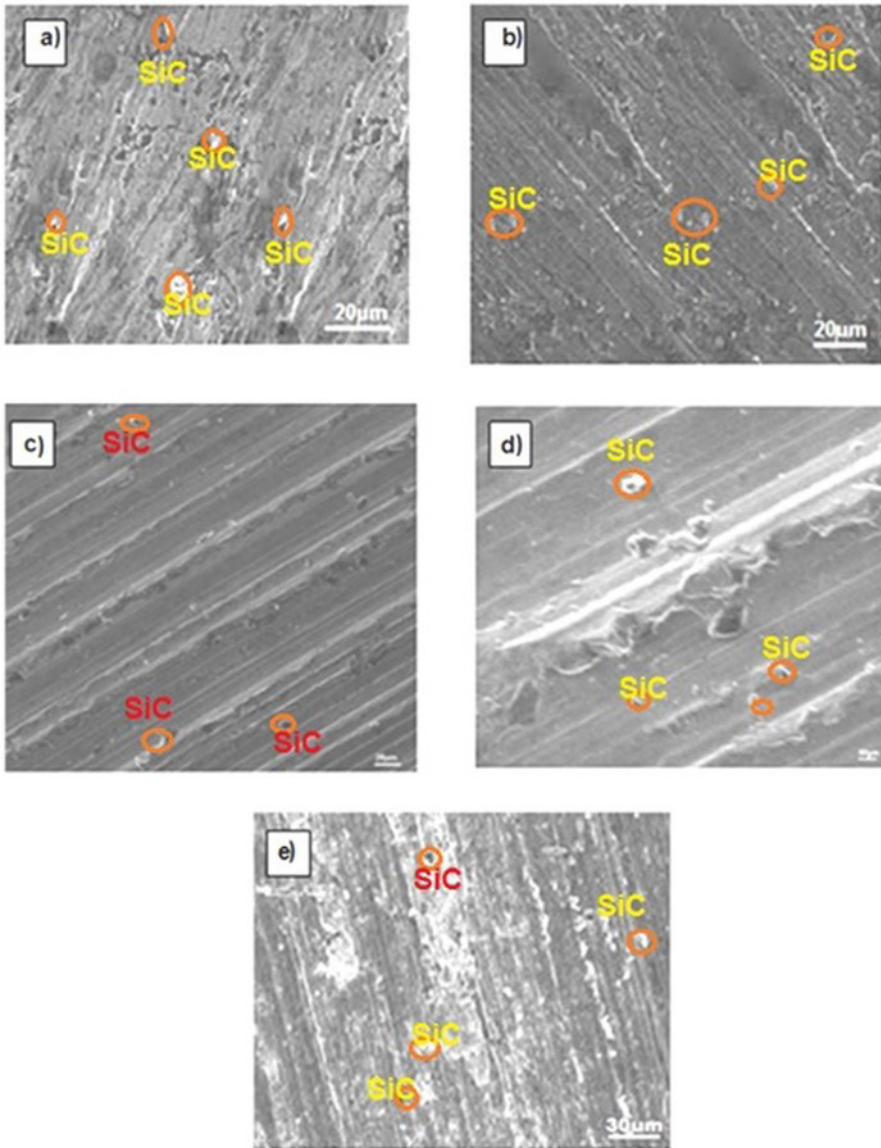


**Figure 5.** SEM images of different worn surfaces (a) 25N of Load, 400 rpm of disc speed, 9m/s of velocity and wear rate of 0.0587 mm<sup>3</sup>/min (b) 20N of Load, 800 rpm of disc speed, 9 m/s of velocity and wear rate of 0.0534 mm<sup>3</sup>/min (c) 15N of Load, 400 rpm of disc speed, 3 m/s of velocity and wear rate of 0.01355 mm<sup>3</sup>/min (d) 20N of Load, 400 rpm of disc speed, 6 m/s of velocity and wear rate of 0.0486 mm<sup>3</sup>/min (e) 25N of Load, 1200 rpm of disc speed, 6 m/s of velocity and wear rate of 0.0893 mm<sup>3</sup>/min.

**Table 3.** Surface texture characteristics for the wear specimens.

Sl.No	Parameters	Values in nm (Nano meters)					Std. Deviation
		Specimen -1	Specimen -2	Specimen -3	Specimen -4	Specimen -5	
1	Roughness Average ( $R_a$ )	34.04	27.66	15.27	17.49	43.12	10.35
2	Root mean square roughness ( $R_q$ )	47.79	37.95	22.29	22.12	56.76	13.74
3	Maximum height of the roughness ( $R_t$ )	350.2	269.1	296.2	178	376.9	69.44
4	Maximum roughness Valley depth ( $R_v$ )	224.7	124.1	129.7	89.39	188.3	48.57
5	Maximum roughness Peak height ( $R_p$ )	125.5	145	166.5	88.61	188.5	34.32
6	Skewness ( $R_{sk}$ )	-0.8543	0.3263	0.9655	0.02416	0.0761	0.586
7	Kurtosis ( $R_{ku}$ )	6.422	4.46	13.39	3.389	3.589	3.727

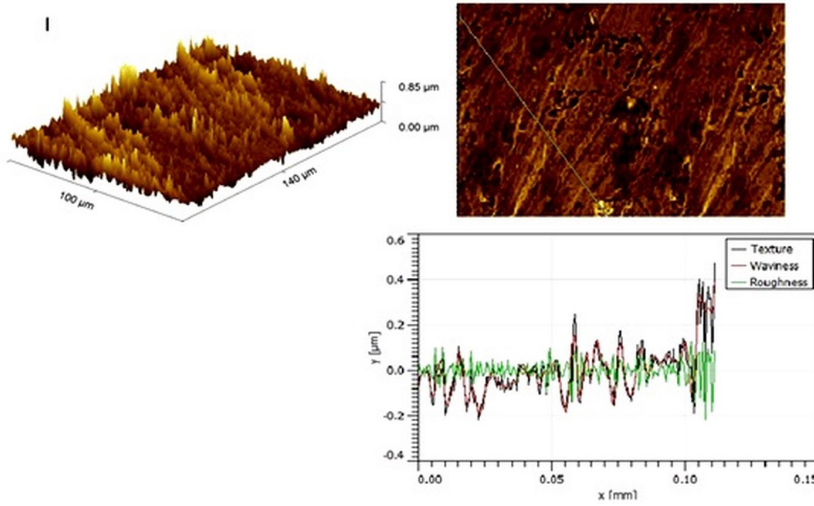


**Figure 6.** AFM images for the specimen1 (25N of Load, 400 rpm of disc speed, 9 m/sec of velocity and wear rate of 0.0587 mm<sup>3</sup>/min).

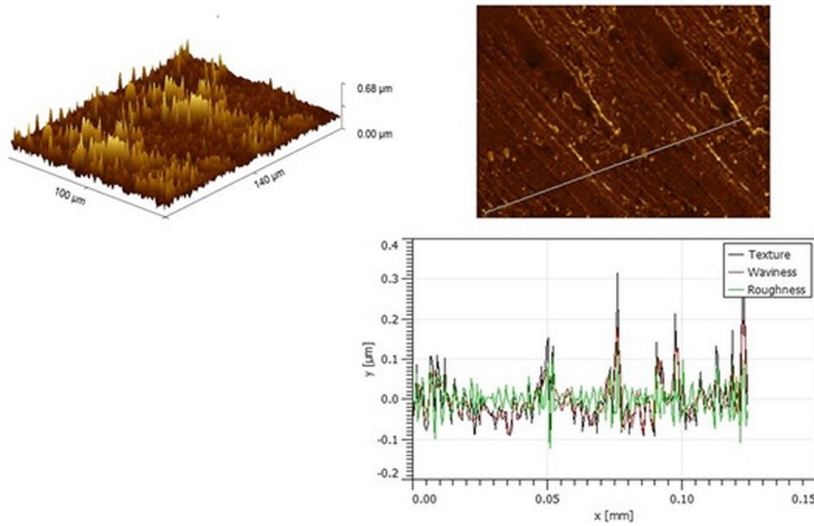


**Figure 7.** AFM images for the specimen 2 (20N of Load, 800 rpm of disc speed, 9 m/sec of velocity and wear rate of 0.0534 mm<sup>3</sup>/min).

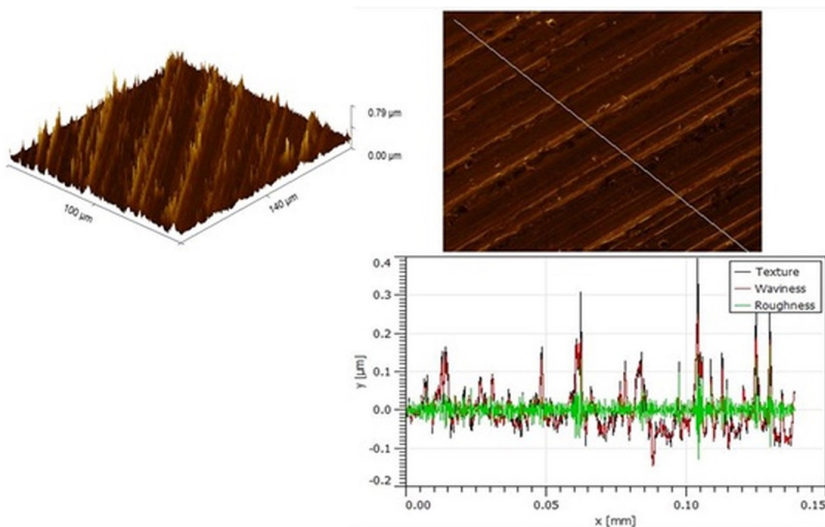


**Figure 8.** AFM images for the specimen 3 (15N of Load, 400 rpm of disc speed, 3 m/sec of velocity and wear rate of 0.01355 mm<sup>3</sup>/min).

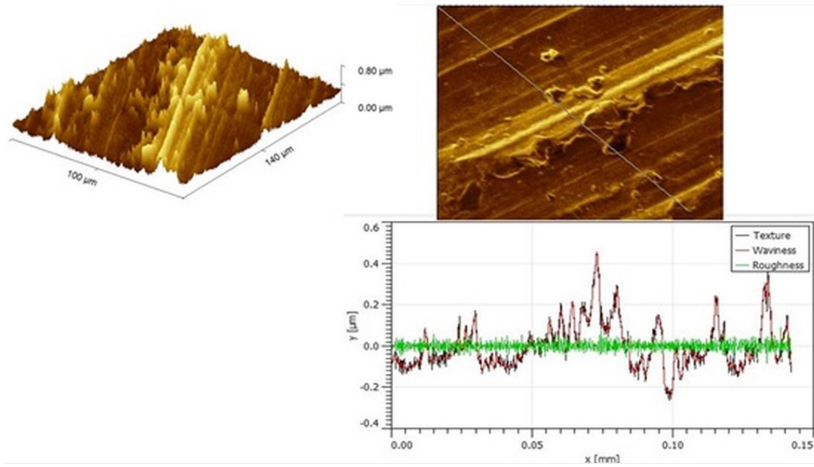


**Figure 9.** AFM images for the specimen 4 (20N of Load, 400 rpm of disc speed, 6 m/sec of velocity and wear rate of  $0.0486 \text{ mm}^3/\text{min}$ ).

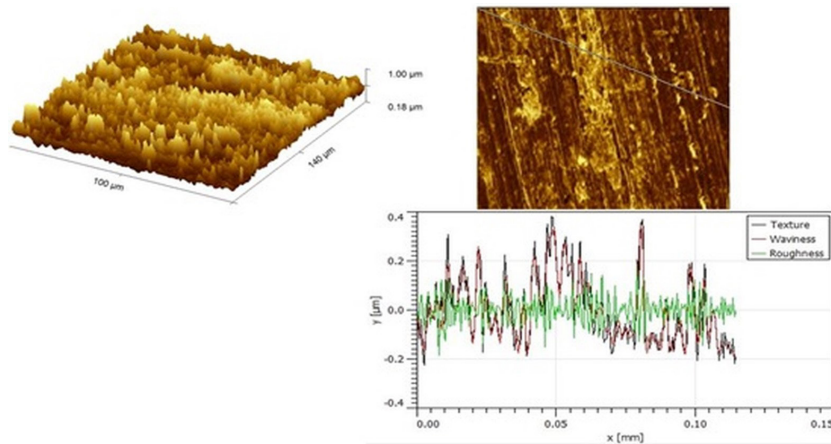


**Figure 10.** AFM images for the specimen 9 (25N of Load, 1200 rpm of disc speed, 6 m/sec of velocity and wear rate of  $0.0893 \text{ mm}^3/\text{min}$ ).

roughness of the surface to the root mean square value is around 1.31 for confirming engineering surfaces, and it follows the Gaussian normal distribution. The kurtosis value for all 5 specimens is above 3, which clearly represents how surface roughness affects wear rate<sup>26-28</sup>. The average roughness measuring method was effectively used by AFM, and it was very useful to investigate the specimen before it went to the manufacturing process. Average roughness and the maximum height of the roughness are the two important parameters to characterize the surface topography of the specimen. In this research, specimen 3 has a minimum average roughness value of 15.27 nm, and specimen 4 has a minimum Rt value of 178 nm, as found in 3D AFM. Similar results were attained in nanoparticles based aluminium composite<sup>29,30</sup>.

#### 4. Conclusion

The following points were presented in conclusion based on the experimental investigation of wear-worn surface analysis on synthesized brass composites.

- A silicon carbide-reinforced brass-based composite was fabricated by the stir casting method. The chemical composition was validated by an EDS image.
- Synthesized brass composite has better mechanical properties, such as a hardness of 510BHN, 8.6 g/cc of density, and 475 MPa of tensile strength.
- The wear characteristics were analyzed with a pin-on-disc tribometer. The wear rate was evaluated by different control factors, such as 15–25 N of applied load, 400–1200 rpm of disc rotational speed, and 3–9 m/s of velocity.
- Based on the input constraints and their level, the wear rate varied from 0.0135 to 0.0893  $\text{mm}^3/\text{min}$
- Load has produced 83.75% of its effect on wear rate. The contributions of disc speed and velocity to wear rate are 14.96% and 1.06%, respectively.
- Atomic force microscopy was used to analyze the wear surface of the brass composite under different loads, disc speeds, and velocities.
- From the surface analysis, the third specimen has a better surface roughness value (27 nm).

## 5. References

- Alkarkhi N, Naif M. Study on the parameter optimization in magnetic abrasive polishing for brass plate using Taguchi method. *Iraqi J Mech Mater Eng*. 2012;12:596-615.
- Alotaibi JG, Yousif BF, Yusaf TF. Wear behaviour and mechanism of different metals sliding against stainless steel counterface. *Proc Inst Mech Eng Part J J Engineer Tribology*. 2014;228(6):692-704.
- Senhadji S, Belarifi F, Robbe-Valloire F. Experimental investigation of friction coefficient and wear rate of brass and bronze under lubrication conditions. *Tribology Ind*. 2016;38:102-7.
- Chowdhury MA, Nuruzzaman DM, Mia AH, Rahaman ML. Friction coefficient of different material pairs under different normal loads and sliding velocities. *Tribology Ind*. 2012;34:18-23.
- Marichamy S, Babu KV, Madan D, Ganesan P. Ultrasonic machining and fretting wear of synthesized duplex brass metal matrix. *Mater Today Proc*. 2020;21:734-7.
- Tabandeh-Khorshid M, Omrani E, Menezes PL, Rohatgi PK. Tribological performance of self-lubricating aluminum matrix nanocomposites: role of graphene nano platelets. *Eng Sci Technol Int J*. 2016;19(1):463-9.
- Vairamuthu J, Velmurugan P, Manohar NJ, Kannan CR, Manivannan S, Stalin B. Wear experimentation and parametric optimization on synthesized copper titanium composite. *Mater Sci Eng*. 2020;1:988-98.
- Jabinth J, Selvakumar N. Enhancing the mechanical, wear behaviour of copper matrix composite with 2V-Gr as reinforcement. *Proc Inst Mech Eng Part J J Engineer Tribology*. 2020;235(7):1405-19.
- Alaneme KK, Odoni BU. Mechanical properties, wear and corrosion behavior of copper matrix composites reinforced with steel machining chips. *Eng Sci Technol Int J*. 2016;19(3):1593-9.
- Sharma VK, Singh RC, Chaudhary R. An experimental study of tribological behaviours of aluminium- and copper-based metal matrix composites for bearing applications. *Int J Mater Eng Innov*. 2019;10(3):1-10.
- Abdoos H, Memar S, Riahi MR. An examination of microstructure, mechanical and dry wear properties of stir cast brass/Al<sub>2</sub>O<sub>3</sub> composites. *Can Metall Q*. 2021;60(2):97-110.
- Wang L, Li DY. Mechanical, electrochemical and tribological properties of nanocrystalline surface of brass produced by sandblasting and annealing. *Surf Coat Tech*. 2003;167(2-3):188-96.
- Zhang G, Liao H, Li H, Mateus C, Bordes JM, Coddet C. On dry sliding friction and wear behaviour of PEEK and PEEK/SiC-composite coatings. *Wear*. 2006;260(6):594-600.
- Li J, Liao H, Coddet C. Friction and wear behaviour of flame sprayed PEEK coatings. *Wear*. 2002;252:824-31.
- So H. Characteristics of wear results tested by pin-on-disc at moderate to high speeds. *Tribology Ind*. 1996;29(5):415-23.
- Ravindranath BS, Murthy BRN, Ramu HC. Process parameters optimization of pin and disc wear test to minimize the wear loss of general-purpose aluminium grades by Taguchi and simulation through response surface methodology. *Eng Sci*. 2020;16:366-73.
- Tyagi R, Xiong D, Li J. Effect of load and sliding speed on friction and wear behavior of silver/h-BN containing Ni-base P/M composites. *Wear*. 2011;270(7-8):423-30.
- Oliveira MD Jr, Costa HL, Silva W Jr, Mello JDB. Effect of iron oxide debris on the reciprocating sliding wear of tool steels. *Wear*. 2019;426:1065-75.
- Palanikumar K, Rajkumar SE, Pitchandi K. Influence of primary B<sub>4</sub>C particles and secondary mica particles on the wear performance of Al6061/B<sub>4</sub>C/mica hybrid composites. *J Bio- Tribo-Corros*. 2019;5(3):1-12.
- Tabrizi AT, Aghajani H, Laleh FF. Tribological characterization of hybrid chromium nitride thin layer synthesized on titanium. *Surf Coat Technol*. 2021;419:127-33.
- Rao GS, Prasad VVSH, Kumar MS. Friction and wear analysis of brass and EN-8 materials. *AIP Conf Proc*. 2021;2417(1):1-10.
- Manimaran P, Kumar KSS, Prithiviraj M. Investigation of physico chemical, mechanical and thermal properties of the albizialebeck bark fibers. *J Nat Fibers*. 2021;18(8):1151-62.
- Manimaran P, Senthamaraiannan P, Sanjay MR, Marichelvam MK, Jawaid M. Study on characterization of *Furcraeafoetida* new natural fiber as composite reinforcement for lightweight applications. *Carbohydr Polym*. 2018;181:650-8.
- Kovács D, Dobránszky J, Bonyár A. Effect of different active screen hole sizes on the surface characteristic of plasma nitrided steel. *Results Phys*. 2019;12:1311-8.
- Arthanarieswaran VP, Kumaravel A, Saravanakumar SS. Physico-chemical properties of alkali-treated *Acacia leucophloea* fibers. *Int J Polym Anal Charact*. 2015;20(8):704-13.
- Li Y, Yang J, Pan Z, Tong W. Nanoscale pore structure and mechanical property analysis of coal: an insight combining AFM and SEM images. *Fuel*. 2020;260:11-21.
- Kumar BR, Hymavathi B, Rao TS. XRD and AFM studies on nanostructured zinc aluminum oxide thin films prepared by Multi-Target magnetron sputtering. *Mater Today Proc*. 2017;4:8638-44.
- Meireles AB, Bastos FDS, Cornacchia TP, Ferreira JA, Las Casas EBD. Enamel wear characterization based on a skewness and kurtosis surface roughness evaluation. *Biotribology*. 2015;1-2:35-41.
- Rajmohan T, Palanikumar K, Arumugam S. Synthesis and characterization of sintered hybrid aluminium matrix composites reinforced with nano copper oxide particles and microsilicon carbide particles. *Compos B Eng*. 2014;59:434-44.
- Faraji G, Asadi P. Characterization of AZ91/alumina nano composite produced by FSP. *Mater Sci Eng A*. 2011;528(6):2431-40.